processes

MDPI

Article

The Effect of Chromium on the Microstructure and Transparency of Diamond-like Carbon Films

Vilius Dovydaitis [1,*], Mindaugas Milieška [2], Johnny Chimborazo [3], Enrico Gnecco [4] and Liutauras Marcinauskas [1,2]

1 Department of Physics, Kaunas University of Technology, Studentų str. 50, 51368 Kaunas, Lithuania; liutauras.marcinauskas@ktu.lt
2 Plasma Processing Laboratory, Lithuanian Energy Institute, Breslaujos str. 3, 44403 Kaunas, Lithuania; mindaugas.milieska@lei.lt
3 School of Physical Sciences and Nanotechnology, Yachay Tech University, Urcuquí 100119, Ecuador; jchimborazo@yachaytech.edu.ec
4 M. Smoluchowski Institute of Physics, Jagiellonian University, Lojasiewicza 11, 30-348 Krakow, Poland; enrico.gnecco@uj.edu.pl
* Correspondence: viliusdovydaitislt@gmail.com

Abstract: Cr-doped diamond-like carbon (DLC) films were formed on silicon and glass substrates by magnetron sputtering (MS). The surface morphology, elemental composition, bonding structure, and transparency of the as-deposited films were analyzed by atomic force microscopy (AFM), the energy-dispersive X-ray spectroscopy (EDS), multiwavelength micro-Raman spectrometer, and UV-VIS-NIR spectrophotometer. The study revealed that the oxygen concentration in the Cr-DLC films increased as the Cr content increased. The surface roughness of the films was slightly reduced when the Cr content was ~9.2 at.%, and further increase in the Cr content up to 13.1 at.% stimulated the growth of the highest-roughness Cr-DLC films. The micro-Raman analysis showed that the G peak position shifted to a higher wavenumber, and the sp^2 bond fraction increased as the Cr concentration in the DLC films rose. The optical transmittance of the Cr-DLC films was reduced by up to 30% compared to DLC coatings due to the increased graphitization process caused by chromium addition.

Keywords: chromium; diamond-like carbon; Raman spectroscopy; magnetron sputtering; oxygen

Received: 3 March 2025
Revised: 21 March 2025
Accepted: 1 April 2025
Published: 6 April 2025

Citation: Dovydaitis, V.; Milieška, M.; Chimborazo, J.; Gnecco, E.; Marcinauskas, L. The Effect of Chromium on the Microstructure and Transparency of Diamond-like Carbon Films. *Processes* **2025**, *13*, 1098. https://doi.org/10.3390/pr13041098

1. Introduction

Diamond-like carbon (DLC) films are widely used in various fields such as automotive, biomedical, optical, and industrial tooling industries due to the high hardness, excellent wear resistance, low coefficient of friction, biocompatibility, optical transparency, etc. [1–3]. It was observed that relatively high residual stress, insufficient adhesion, or low oxidation and thermal resistance limit the application fields of DLC films [2–5]. The final properties of the synthesized DLC films are highly related to the sp^2 carbon and C-C bonds ratio and the concentration of the dopants [1,3,6,7].

It was found that metal (Ti, Cr, Ni, Mo, Ag, Cu) or non-metal (Si, O, N, F) doping of the DLC films allows us to modify the structure, improve the adhesion, wear resistance, and thermal stability, reduce internal stress, enhance thermal conductivity, and control the optical and electrical properties [6–9]. Chromium-doped DLC films are advanced nanocomposite coatings that combine the exceptional hardness and low friction properties of DLC films with the enhanced mechanical and tribological performance provided by

chromium doping [8,10–17]. J.A. Santiago et al. [8] showed that adding more chromium enhanced the sp^2 bond fraction and reduced the hardness and friction coefficient of the DLC films. W. Dai et al. [10] observed that films with a low Cr doping concentration exhibited excellent tribological properties, but the friction coefficient and wear rates were slightly higher than those of pure DLC films. J. Zheng et al. [11] found that an increase in the Cr concentration from 7.7 at. % to 11.2 at. % enhanced the surface roughness, sp^3 bond fraction, Cr-C sites concentration, and nano-hardness of the DLC films. As a result, the tribological properties of the Cr-DLC films were improved. A. Khodayari et al. [12] indicated that an increase in the Cr concentration enhanced the surface roughness, improved wear resistance and elasticity modulus, but reduced the hardness and adhesion strength of hydrogenated DLC films. L. Wang et al. [13] observed that the reduction in the Cr content from 3.3 at.% to 1.22 at.% increased the sp^3 bond content, reduced Cr-C sites fraction, while the oxygen concentration was ~7 at.% in the thin DLC films. C.W. Zou et al. [14] showed that the increase in the Cr content from 2 to 9.7 at. % reduced the hardness from 22.7 GPa to 12.5 GPa in the DLC films, respectively. Meanwhile, the coefficient of friction of the Cr-DLC films was minimized due to the increase in the sp^2/sp^3 ratio. W. Dai et al. [15] demonstrated that the sp^2 C=C bond fraction and surface roughness increased with the increase in Cr concentration from 1.5 to 40.1 at.%, respectively. According to S. Viswanathan et al. [16], a rise in Cr concentration resulted in a lower sp^3/sp^2 bond ratio and hardness, while enhancing the formation of Cr-C and Cr-O bonds in greater amounts within the films. The wear resistance and corrosion resistance properties of DLC films were improved with an addition of low concentration (3.8 at. %) of chromium. The Cr-doped DLC films with a low concentration demonstrated an improved tribological properties, compared to pure DLC film [10]. Y. Zhuang et at. [17] indicated that the corrosion properties of the Cr-DLC films were improved with the reduction in sp^3 bond fraction. The tribological properties of the DLC films are controlled by the addition of different concentrations of chromium [18]. The rise in the Cr quantity reduced the sp^3 bond proportion and heightened the wear rate of the Cr-DLC films [19]. The increase in the Cr content from 1.96 to 17.21 at.% enhanced the hardness of the DLC films from 5.72 to 8.02 GPa, respectively. However, the graphitization and formation of chromium carbides promoted higher friction coefficient and wear rates of the films [20].

Various researchers demonstrated that the optical transmittance of DLC or doped DLC films in the UV-VIS-IR wavelength range is highly dependent on the sp^2 to sp^3 ratio [21–27]. E. Mohammadinia et al. [21] determined that the transmission of Ni-doped a-C:H films in VIS-IR range was reduced due to the enlargement in the sp^2 sites with the enhancement of Ni content. B. Zhou et al. [22] showed that the rise in the Cu content from 8.3 wt.% to 27.9 wt.% reduced the sp^3 fraction from 55.6% to 36.0% and drastically reduced the optical transmittance of Cu-DLC films. When the Cu concentration was 12.6 wt.%, the transmittance of the film in the VIS-NIR range was lower than 40%. Meanwhile, the Cu-DLC film with 27.9% of Cu was opaque to UV wavelengths, and the transmittance was only 10% in the VIS range. The optical transmittance in the range of 300 to 2500 nm decreased with enhancement in the deposition temperature of DLC films. This was attributed to temperature-induced graphitization of the DLC coatings [23]. Š. Meškinis et al. [24] demonstrated that the addition of the Si and O increased the transparency of the DLC coatings due to increase in the sp^3 bond fraction. M. Qi et al. [25] found that the hafnium- and nitrogen-co-doped DLC films showed a lower transmittance due to the reduction in sp^3 bond content. W. Kijaszek et al. [26] obtained a shift of the absorption edge in the transmittance spectra of DLC films from ~255 nm to ~285 nm with the increase in the sp^3 content. N. Boubiche et al. [27] indicated that the optical transparency was reduced

with the addition of Ni and annealing of Ni-DLC and DLC coatings. The reduction in the transmittance of films was assigned in the growth of graphitic cluster amount.

A literature analysis demonstrated that the final properties of Cr-DLC coatings depend not only on the Cr concentration, but also on the choice of deposition technique used. Even a small change in process parameters can significantly vary the concentration of sp^2/sp^3 bonds ratio in the DLC films and thereby control the mechanical, optical, tribological or corrosion properties of the coatings. It is important to mention that there are almost no data about the transmittance values of Cr-DLC films in the scientific literature.

The DLC and chromium-doped DLC films were formed by magnetron sputtering. The aim of the work was to determine the effect of the chromium concentration on the elemental composition, surface roughness, structure, and optical transparency of DLC films.

2. Materials and Methods

Direct current magnetron sputtering was used to deposit chromium-doped amorphous carbon films onto silicon (100) and glass substrates [28]. Three-inch-diameter disc targets containing 99.99% pure chromium (Kurt J. Lesker Company, Saint Leonards, UK) and 99.9% pure graphite were used. The substrates were located at 60 mm distance from the magnetrons. Using a substrate moving periodically and parallel to the cathodes' motion over magnetrons, the formation was achieved. The cathodes were etched for 5 min in Ar plasma at 2–3 Pa after the chamber was pumped to a pressure of less than 0.01 Pa. The graphite and chromium target currents were set at 1.5 A and 0.5 A, respectively. The synthesis was conducted with argon at a pressure of 2–3 Pa, and the formation lasted for 10 min. The films had a thickness between 220 nm and 250 nm.

For the elemental composition analysis of the deposited films, the energy-dispersive X-ray spectroscopy (EDS) (Bruker Quad 5040 spectrometer, AXS Microanalysis GmbH, Hamburg, Germany) was performed. A surface area of 1.25 mm^2 was measured using 15 kV accelerating voltage at five different points, and the mean values were computed. The micro-Raman spectroscopy (Horiba Jobin Yvon LabRAM HR system, HORIBA, Ltd., Kyoto, Japan) was used to determine the bonding structure of the DLC and Cr-DLC films. Raman spectra were recorded at room temperature within the spectral range of 1000–1800 cm^{-1} using three distinct lasers with wavelengths of 458 nm (0.5 mW), 514 nm (0.5 mW), and 633 nm (0.45 mW). The Raman spectra of the films were fitted using two Gaussian-shaped lines within the 1000–1800 cm^{-1} spectral range in Microcal Origin 8 software. The films' transmittance spectra were captured between 400 and 1300 nm wavelengths using a Shimadzu UV-3600 UV-VIS-NIR spectrophotometer (Shimadzu, Kyoto, Japan). Detailed information on the characterization of the films is given in ref. [28,29]. Atomic force microscopy (AFM) (Nanowizard 4, JPK Instruments, Berlin, Germany) was used to examine the surface roughness of the Cr-doped DLC films.

3. Results and Discussions

The elemental composition measurements showed that the Cr content was enhanced with the increase in the split width. The Cr-DLC15 film was composed of chromium, oxygen, and carbon with a concentration of 7.4 at. %, 34.6 at. %, and 58.0 at.%, respectively. The chromium amount in the coating increased to 9.2 at.%, while the oxygen content was enhanced to 39.1 at.% with the increase in the slit width from 13 mm to 22 mm, respectively. The highest concentrations of the Cr and O were obtained in the Cr-DLC17 film and were 13.1 at. % and 51.0 at.%, respectively. The DLC film without the Cr contained ~25.3 at. % of the oxygen. The obtained results indicate that chromium reacted actively with oxygen due to the large difference in electronegativity. The electronegativity of chromium is 1.66, and that of oxygen is 3.44 [28]. Therefore, it is likely that chromium oxides were formed

in the DLC films when chromium was sputtered and reached the substrate. Most authors argue that the appearance of oxygen in the DLC coatings is due to two reasons: derived from the residual air left in the vacuum chamber, and formation of the chromium oxides and carbon oxides after the exposure of the DLC films in air [11,13,30–34]. According to Y. S. Park et al. [30], the oxygen content in metal-doped a-C films ranges from 10 to 30 at.% depending on the specific metal used. Z. Wu et al. [31] observed that the Cr-DLC coating with the chromium concentration of ~2 at.% contained huge concentration (~18 at.%) of oxygen. The contamination of Cr-DLC films with oxygen was primarily attributable to the adsorption of oxygen from the atmosphere. As a result, the generation of the C-O, C=O, and Cr-O bonds was induced in the Cr-DLC films [13]. K. Jastrzebski et al. [32] observed that the free bonds created on the surface of the DLC films are rapidly saturated with oxygen from the atmosphere during chamber aeration. Several authors demonstrated the formation of Cr-O bonds in the Cr-DLC films [11,13,33,34]. The oxygen content in the Cr-doped DLC coatings was from 2 at.% to ~6 at.% and depended on the used bias voltage. L. Wang et al. [13] indicated that the oxygen content was about ~7 at. in the Cr-DLC films when the chromium amount varied from 1.2 at to 3.2 at. H. Dong et al. [33] observed that the oxygen content in the Cr/N-doped DLC films was in the range of 13.4 to 19.0 at. %. The quantity of oxygen rose with the rise in Cr amount in the coatings. As the Cr target power was increased, more Cr atoms were produced, and a higher fraction of chromium was bonded to the oxygen during the film deposition.

The surface of chromium-doped DLC films was composed of grains with sizes ranging from 30 nm to 50 nm. The increase in the Cr content almost did not affect the structure of the films (Figure 1). The variation in the roughness of DLC films versus the chromium concentration is presented in Figure 2. The average surface roughness (R_a) and the root mean square roughness (R_q) of the DLC film were 1.82 nm and 2.30 nm, respectively. The Cr doping of the DLC films firstly decreased the surface roughness; when the chromium concentrations increased to a certain critical value, the surface roughness of the films were enhanced. The R_a and R_q values of the Cr-DLC15 film were 1.72 nm and 2.18 nm, respectively. The further increase in the Cr content to 9.2 at.%, led to a slight reduction in the roughness of the surface to 1.63 nm and 2.07 nm. The Cr-DLC film with the highest concentration of the chromium demonstrated the highest R_a and R_q values of 2.05 nm and 2.70 nm, respectively. P. Pisarik et al. [35] observed that when DLC coatings were doped with chromium, the average roughness of the coatings rose from 0.62 nm to 1.04 nm, with the increase in the Cr content from 2.2 at.% to 17.9 at.%, respectively. As the concentration of the chromium increased, a slight increase in the agglomerates formed on the surface of the Cr-DLC films was observed [18,35]. The roughness of the Cr-DLC coatings prepared by unbalanced magnetron sputtering depended on the thickness and Cr content in the films [13]. When the Cr-DLC films were deposited, graphite and Cr magnetron targets were used, and the density of the plasma was increased. Thus, the energy of the arriving atoms on the surface was probably higher compared to the energy of carbon atoms when a single graphite target was used. A higher energy of arriving atoms will increase the diffusion of adatoms on the surface and will stimulate the formation of more flattened and denser coating. Such phenomena were observed for Cr-DLC15 and Cr-DLC16 films. However, when the Cr concentration increased further up to 13.1 at.%., the small particles agglomerated and grew into larger-size clusters. Consequently, the roughness of the Cr-DLC17 film grew. Additionally, as the chromium concentration increased, a slight increase in the films thickness was observed [13]. A reduction in the roughness of the surface with an addition of a low amount of Cr was observed in Cr/N-DLC films [33]. Meanwhile, W. Dai et al. [15] observed that the enlargement in the surface roughness of the Cr-DLC

coatings was attributed to the formation of large quantities of chromium carbides with the enhancement of the chromium amount in the diamond-like carbon coatings.

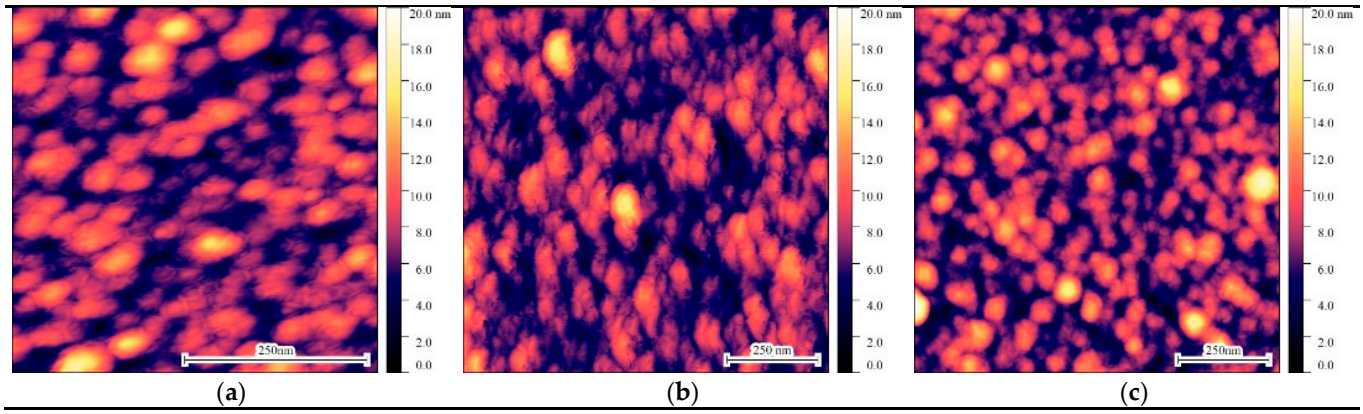

Figure 1. AFM topographical views of the films: (**a**) Cr-DLC15, (**b**) Cr-DLC16, and (**c**) Cr-DLC17.

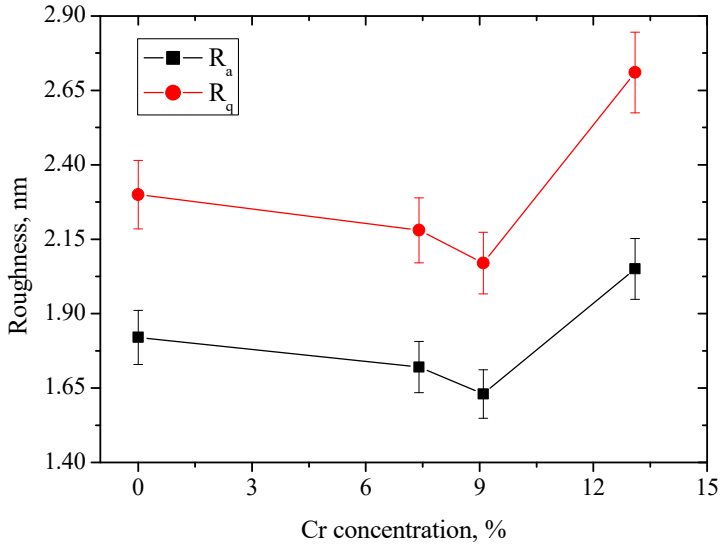

Figure 2. Variation in the roughness of the coatings versus the chromium concentration.

Raman spectra of the chromium-doped DLC films are given in Figure 3. In different DLC films, the extent of structural disorder is indicated by either the ratio of the integrated intensity of the D peak to the G peak (I_D/I_G) or the ratio of their integrated areas (A_D/A_G) [1,14]. Information about the sp^2 site fraction and the structure of the DLC films can also be derived from the G peak position and the full width at half maximum ($FWHM_G$) of the G band. The increase in the laser wavelength led to an increase in the I_D/I_G and A_D/A_G ratios for all deposited films. The estimated I_D/I_G and A_D/A_G ratios of the DLC1 film at an excitation wavelength of 458 nm were 0.41 and 0.92, at a wavelength of 514 nm–0.63 and 1.40, and at a wavelength of 633 nm–0.86 and 1.65, respectively. Adding the lowest Cr content in the film slightly enhanced the I_D/I_G and A_D/A_G ratios. The I_D/I_G and A_D/A_G ratios were enhanced from 0.62 (at 458 nm) to 1.01 (at 633 nm) and from 1.73 (at 458 nm) to 1.87 (at 633 nm), respectively. Meanwhile, the A_D/A_G and I_D/I_G ratios for the Cr-DLC film with the highest concentration of chromium, accordingly, increased from 1.32 to 2.47 and from 0.55 to 1.12 with the enhancement in the laser wavelength, respectively. The Raman spectra results indicated that the A_D/A_G and I_D/I_G ratio values were enhanced with increased chromium concentration and the laser wavelengths. The enhanced intensity of the D peak is due to the creation of a higher fraction of aromatic disordered rings

and an increase in the sp^2 C=C content in the Cr-DLC coatings leading to higher I_D/I_G ratios [11,14–16,28]. The enlargement in the I_D/I_G ratio is linked with the enhancement in the fraction of the sp^2 C=C sites in chromium-doped DLC films [15,19,36,37].

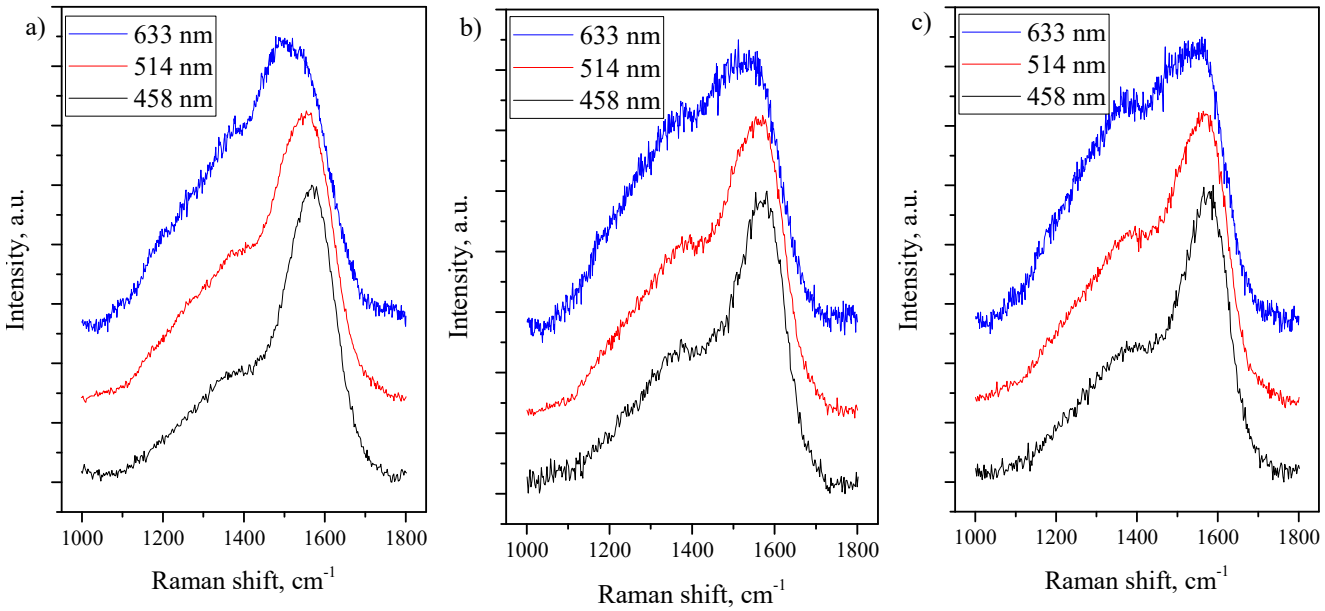

Figure 3. Raman spectra of the (**a**) Cr-DLC15, (**b**) Cr-DLC16, and (**c**) Cr-DLC17 films measured using various laser wavelengths.

The results of Raman spectra measured at different laser wavelengths showed that the position of the G peak moved to lower values as the wavelength increases from 458 nm to 632 nm (Figure 4). The lowest G band position values were obtained in the DLC1 film. The G peak was located at 1570 cm^{-1}, 1559 cm^{-1} and 1534 cm^{-1}, when measurements were performed with 458 nm, 514 nm and 633 nm wavelength lasers, respectively. Despite the relatively high oxygen content in the films, the Raman spectra of Cr-DLC films retained the shape typical of DLC coatings (Figure 3). The location of the G peak in the Cr-DLC15 film moved from 1548 cm^{-1} to 1577 cm^{-1}, while in the Cr-DLC16 and Cr-DLC17 films, the G peak moved from 1547 cm^{-1} to 1574 cm^{-1}, and from 1557 cm^{-1} to 1576 cm^{-1}, with the respective reduction in the laser wavelength (Figure 4). The dispersion of the *G* band (D_G) was calculated by the methodology presented in the work by A. Assembayeva et al. [38].

$$D_G = \frac{G_{458} - G_{633}}{\lambda_{633} - \lambda_{458}} \quad (1)$$

where λ_{633} and λ_{458} are wavelengths of used laser at 633 nm and 458 nm, respectively. G_{458} and G_{633} are the *G* peak positions of the films determined from the Raman spectra obtained using laser with 458 nm and 633 nm, respectively.

The D_G value gives information about the structural changes and sp^2 bonding trend in the diamond-like carbon coatings. The calculations demonstrated that the DLC film showed a D_G parameter equal to ~0.206 cm^{-1}/nm. The D_G value was reduced to 0.167 cm^{-1}/nm when the Cr concentration was 7.4 at.%. The rise in the chromium content within the film to 9.2 at.% resulted in a slight reduction in the D_G value to 0.154 cm^{-1}/nm. The most minimal (~0.109 cm^{-1}/nm) dispersion data were observed for Cr-DLC17 film with the highest concentration of the chromium. The G band position was up-shifted to higher values in the Cr-DLC with the reduction in the laser's excitation from 633 nm to 488 nm [37]. The reduction in the D_G value from 0.206 to 0.109 cm^{-1}/nm is direct evidence of the enhanced clustering of the rings in the structure of DLC films [37,38]. A. Assembayeva et al. [38]

observed that the dispersion of the G band decreased from 0.34 to 0.24 cm^{-1}/nm with the enhancement in the palladium quantity from 0.96 at.% to 5.58 at.% in the DLC films, respectively. The reduction in the D_G values was assigned to the increase in the sp^2 bond fraction and promoted graphitization in the Pd-DLC films. The higher the dispersion values, the more disordered is the sp^2 carbon network formed. The graphite or carbon films with a high fraction of sp^2 C=C sites have only minor dispersion of the G peak values [28,37,38].

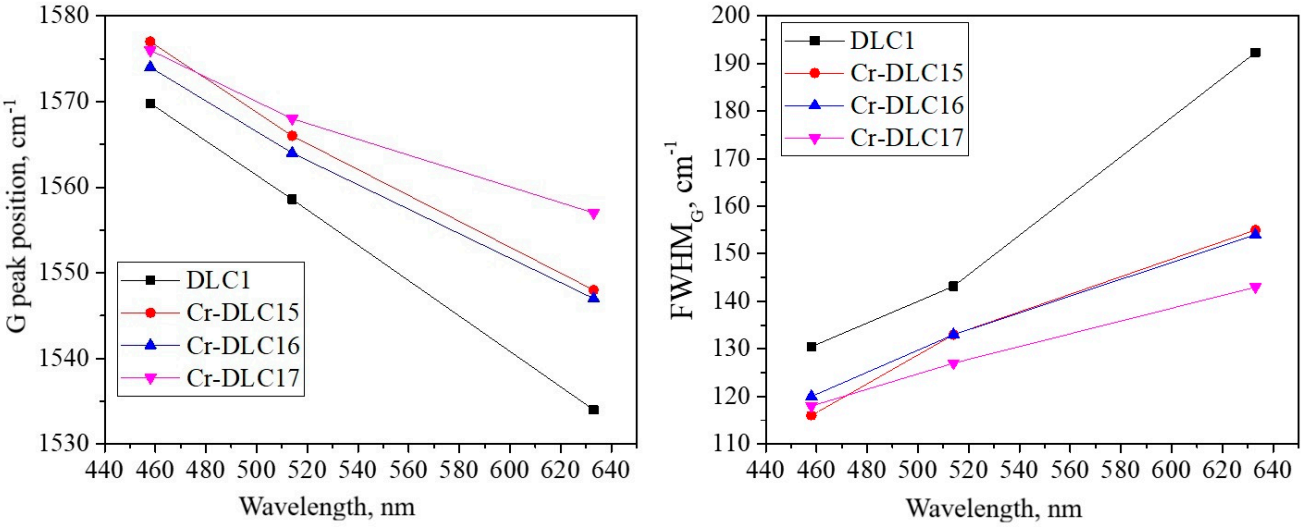

Figure 4. The dependence of G peak position (**left**) and $FWHM_G$ values in DLC and Cr-DLC films under various laser excitation wavelengths.

The highest values of the full width at half maximum of the G peak were observed for DLC1 film (Figure 4). However, the $FWHM_G$ value broadened from 131 cm^{-1} to 176 cm^{-1} with increased wavelengths. The $FWHM_G$ of the G peak for the Cr-DLC15 film was enhanced from 116 cm^{-1} to 155 cm^{-1}, with increase in the laser wavelength. The increase in the Cr concentration to 9.2 at.% only slightly changed the $FWHM_G$ values. The $FWHM_G$ value increased from 120 cm^{-1} to 154 cm^{-1}, respectively, when 458 nm and 633 nm laser excitations were used. The narrowest G peak was observed in the DLC films when the highest amount of Cr was used (Figure 4). However, as the laser wavelength increased, the $FWHM_G$ values broadened from 118 cm^{-1} to 143 cm^{-1}, respectively.

As the size of the nano-graphite clusters increases and the sp^2 bond fraction is enhanced, the position of the G band shifts to higher wavenumbers [36]. D. Savchenko et al. [37] obtained an increase in the I_D/I_G ratio with both the Cr concentration and laser wavelength. Those trends are similar to those observed in our research. The G peak position was found to move upward steadily with rising chromium amounts, suggesting that the sp^2/sp^3 ratio increased with the Cr content [14,37]. Several authors [14,16,18,37] have noted the rise of sp^2 carbon sites and the induced graphitization in the chromium-DLC coatings. Consequently, the included chromium metal particles behave as catalysts in the creation of C=C carbon sites within an amorphous network of carbon sites [16,37]. S. Viswanathan et al. [16] observed that the enhancement in the Cr concentration reduced the sp^3 C-C sites fraction and induced growth of Cr-C and Cr-O bonds in the Cr-DLC films. M. Evaristo et al. [39] observed that the incorporation of the oxygen in the DLC films reduced the sp^3 sites fraction and enhanced the size of graphitic clusters. L. Wang et al. [13] found that the reduction in Cr content broadened the G peak and reduced I_D/I_G value of the DLC films. with similar oxygen content. B. Mi et al. [40] demonstrated that the increase in the Cr/Ti

co-dopants concentration in the DLC films enhanced the oxygen concentration, shifted the G peak to higher values and increased the I_D/I_G ratio.

The optical transmittance of the as-deposited films is given in Figure 5. The findings suggested that the highest transmittance was observed for the DLC1 film. The increased Cr content reduced the optical transmittance of the formed films (Figure 5). The transmittance of the Cr-doped coatings at 500 nm decreased with increasing the Cr concentration in the films. The transmittance of Cr-DLC15 was 57%, and the optical transmittance values of Cr-DLC16 and Cr-DLC17 films were reduced to 41% and 38%, respectively. It should be mentioned that the optical transmittance of the Cr-DLC film was reduced by ~15% in the whole wavelength range when the Cr content was increased from 7.4 at. % to 9.2 at. % (Figure 5). The results indicated that the optical transmittance of the Cr-DLC16 and Cr-DLC17 films was very similar, despite the difference in the Cr and O concentrations and sp^2/sp^3 bond ratio (Figure 5).

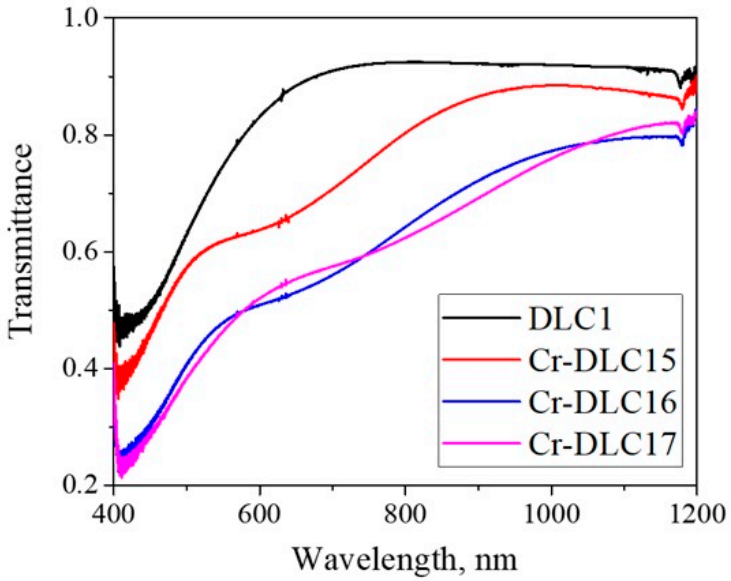

Figure 5. Optical transmittance of the pure and chromium-doped diamond-like carbon films.

It was indicated that silicon and oxygen doping increased the optical transparency of DLC films [24]. E. Braca et al. [41] observed that the transparency of a-C:H films was enhanced with the increase in oxygen concentration. M. Qi et al. [25] obtained that the transmittance of the (Hf:N)-DLC coatings was reduced with the formation of sp^2 phase and the graphitization of the films, due to changes in the nitrogen and Hf content in the films. The transmittance of the films at 400 nm could be reduced from 45% to 25% with an increase in the N_2 flow rate. The authors indicated that the combination of N and C atoms induces an increase in the density of π states, which can increase the optical transparency of the co-doped DLC films. A. Mikhchin et al. [42] discovered that the optical transmittance of Cu-DLC films could be enhanced by 10% in the 400–900 nm wavelength range. The enhanced optical transmittance of Cu-DLC films was linked to the decreased amount and size of copper nanoparticles and the rise in the sp^3 bond quantity. A reduction in the transparency of DLC films was observed when the nitrogen- or boron-doped DLC films were formed [43]. The results indicated that the optical transparency of the DLC films was reduced with the introduction of chromium as the concentration of sp^3 C-C bonds was reduced. However, the increased oxygen content in the films can compensate for the loss of sp^3 bonds and obtain similar transmittance values, which is seen in the case of Cr-DLC16 and Cr-DLC 17 films.

4. Conclusions

The DLC and Cr-DLC films were obtained by magnetron sputtering. An increase in the concentration of chromium from 7.4 at.% to 13.1 at.% enhanced the oxygen quantity in the DLC films from 34.6 at.% to 51.0 at.%, respectively. It is important to note that the oxygen content in the Cr-DLC films was up to twice as high as in the DLC films. The surface roughness of the Cr-DLC films was ~10% lower, when the Cr content was 9.2 at.%. The Raman spectroscopy data demonstrated that the increase in the chromium concentration shifted the G peak to higher values, enhanced the I_D/I_G and A_D/A_G ratios, and narrowed the G band. The dispersion of the G peak was reduced from 0.206 cm^{-1}/nm to 0.109 cm^{-1}/nm with the enhancement of the chromium amount in the films. These findings show that the concentration of sp^2 bonds increased, resulting in the creation of larger graphite clusters with a lower number of defects in the Cr-DLC films. The enlargement in the Cr concentration reduced the optical transparency of the DLC films. It was found that the reduction in the transmittance is due to the enhanced sp^2 C=C bond portion in the Cr-doped DLC films. However, the high content of oxygen in the Cr-DLC films can recover the reduction in the sp^3 C-C sites and deposit films with transmittance values greater than 70% in the infrared wavelength range.

Author Contributions: Conceptualization, L.M. and V.D.; methodology, V.D., M.M. and L.M.; software, J.C., V.D. and E.G.; validation, L.M., V.D. and J.C.; formal analysis, V.D. and M.M.; investigation, V.D., E.G., M.M., L.M. and J.C.; resources, V.D. and L.M.; data curation, V.D.; writing—original draft preparation, V.D. and L.M.; writing—review and editing, V.D. and L.M.; visualization, V.D.; supervision, V.D. and L.M. All authors have read and agreed to the published version of the manuscript.

Funding: This research received no external funding.

Data Availability Statement: The original contributions presented in this study are included in the article. Further inquiries can be directed to the corresponding author.

Acknowledgments: The authors would like to acknowledge the contribution of the COST Action CA15107 (MultiComp) and the COST Action ESSENCe, supported by COST (European Cooperation in Science and Technology). The authors would like to thank Susanne Sandkuhl from Otto Schott Institute of Materials Research (OSIM) for AFM measurements.

Conflicts of Interest: The authors declare no conflicts of interest.

References

1. Ohtake, N.; Hiratsuka, M.; Kanda, K.; Akasaka, H.; Tsujioka, M.; Hirakuri, K.; Hirata, A.; Ohana, T.; Inaba, H.; Kano, M.; et al. Properties and Classification of Diamond-Like Carbon Films. *Materials* **2021**, *14*, 315. [CrossRef] [PubMed]
2. Bewilogua, K.; Hofmann, D. History of diamond-like carbon films—From first experiments to worldwide applications. *Surf. Coat. Technol.* **2014**, *242*, 214–225. [CrossRef]
3. Vetter, J. 60 years of DLC coatings: Historical highlights and technical review of cathodic arc processes to synthesize various DLC types, and their evolution for indus-trial applications. *Surf. Coat. Technol.* **2014**, *257*, 213–240.
4. Sharifahmadian, O.; Pakseresht, A.; Mosas, K.K.A.; Galusek, D. Doping effects on the tribological performance of diamond-like carbon coatings: A review. *J. Mater. Res. Technol.* **2023**, *27*, 7748–7765. [CrossRef]
5. Liu, J.; Yang, T.; Cao, H.; Deng, Q.; Pan, C.; Wen, F. Diamond-like Carbon Films for Tribological Modification of Rubber. *Nanotechnol. Rev.* **2022**, *11*, 2839–2856.
6. Sánchez-López, J.C.; Fernández, A. Doping and Alloying Effects on DLC Coatings. In *Tribology of Diamond-Like Carbon Films: Fundamentals and Applications*; Donnet, C., Erdemir, A., Eds.; Springer: Berlin, Germany, 2008; pp. 311–338.
7. Sun, H.; Yang, L.; Wu, H.; Zhao, L. Effects of Element Doping on the Structure and Properties of Diamond-like Carbon Films: A Review. *Lubricants* **2023**, *11*, 186. [CrossRef]
8. Santiago, J.; Fernández-Martínez, I.; Sánchez-López, J.; Rojas, T.; Wennberg, A.; Bellido-González, V.; Molina-Aldareguia, J.; Monclús, M.; González-Arrabal, R. Tribomechanical properties of hard Cr-doped DLC coatings deposited by low-frequency HiPIMS. *Surf. Coat. Technol.* **2020**, *382*, 124899. [CrossRef]

9. Li, L.; Song, W.; Liu, J.; Liu, Q.; Wang, S.; Zhang, G. Tribology International Nanomechanical and nanotribological behavior of ultra-thin silicon-doped diamond-like carbon films. *Tribiol. Int.* **2016**, *94*, 616–623. [CrossRef]
10. Dai, W.; Wang, A. Synthesis, characterization and properties of the DLC films with low Cr concentration doping by a hybrid linear ion beam system. *Surf. Coat. Technol.* **2011**, *205*, 2882–2886. [CrossRef]
11. Zheng, J.; Shang, J.; Zhuang, W.; Ding, J.C.; Mei, H.; Yang, Y.; Ran, S. Structural and tribomechanical properties of Cr-DLC films deposited by reactive high power impulse magnetron sputtering. *Vacuum* **2024**, *230*, 113611. [CrossRef]
12. Khodayari, A.; Elmkhah, H.; Alizadeh, M.; Maghsoudipour, A. Modified dia-mond-like carbon (Cr-DLC) coating applied by PACVD-CAPVD hybrid method: Characterization and evaluation of tribological and corrosion behavior. *Diam. Relat. Mater.* **2023**, *136*, 109968. [CrossRef]
13. Wang, L.; Wu, Y.; Yu, S.; Liu, Y.; Shi, B.; Hu, E.; Hei, H. Investigation of hydrophobic and anti-corrosive behavior of Cr-DLC film on stainless steel bipolar plate. *Diam. Relat. Mater.* **2022**, *129*, 109352. [CrossRef]
14. Zou, C.; Wang, H.; Feng, L.; Xue, S. Effects of Cr concentrations on the microstructure, hardness, and temperature-dependent tribological properties of Cr-DLC coatings. *Appl. Surf. Sci.* **2013**, *286*, 137–141. [CrossRef]
15. Dai, W.; Ke, P.; Wang, A. Microstructure and property evolution of Cr-DLC films with different Cr content deposited by a hybrid beam technique. *Vacuum* **2011**, *85*, 792–797. [CrossRef]
16. Viswanathan, S.; Mohan, L.; Bera, P.; Kumar, V.P.; Barshilia, H.C.; Anandan, C. Corrosion and Wear Behaviors of Cr-Doped Diamond-Like Carbon Coatings. *J. Mater. Eng. Perform.* **2017**, *26*, 3633–3647. [CrossRef]
17. Zhuang, Y.; Jiang, X.; Rogachev, A.; Piliptsou, D.; Ye, B.; Liu, G.; Zhou, T.; Rudenkov, A. Influences of pulse frequency on the structure and anti-corrosion properties of the a-C:Cr films. *Appl. Surf. Sci.* **2015**, *351*, 1197–1203. [CrossRef]
18. Gayathri, S.; Kumar, N.; Krishnan, R.; Ravindran, T.; Dash, S.; Tyagi, A.; Sridharan, M. Influence of Cr content on the micro-structural and tribological properties of PLD grown nanocomposite DLC-Cr thin films. *Mater. Chem. Phys.* **2015**, *167*, 194–200. [CrossRef]
19. Liu, S.; Zhuang, W.; Ding, J.; Liu, Y.; Yu, W.; Yang, Y.; Liu, X.; Yuan, J.; Zheng, J. Fabrication and Tribological Properties of Diamond-like Carbon Film with Cr Doping by High-Power Impulse Magnetron Sputtering. *Coatings* **2024**, *14*, 916. [CrossRef]
20. Li, G.; Xu, Y.; Xia, Y. Effect of Cr Atom Plasma Emission Intensity on the Characteristics of Cr-DLC Films Deposited by Pulsed-DC Magnetron Sputtering. *Coatings* **2020**, *10*, 608. [CrossRef]
21. Mohammadinia, E.; Elahia, S.M.; Shahid, S. Structural and optical properties of Ni-embedded hydrogenated diamondlike carbon (Ni-DLC) prepared by co-deposition of RF-Sputtering and RF-PECVD method. *Mater. Sci. Semicond. Process.* **2018**, *74*, 7–12. [CrossRef]
22. Zhou, B.; Liu, Z.; Piliptsou, D.; Yu, S.; Wang, Z.; Rogachev, A.; Rudenkov, A.; Balmakou, A. Structure and optical properties of Cu-DLC composite films deposited by cathode arc with double-excitation source. *Diam. Relat. Mater.* **2016**, *69*, 191–197. [CrossRef]
23. Moghadam, R.Z.; Dizaji, H.R.; Ehsani, M.H.; Kameli, P.; Jannesari, M. Correlation study of structural, optical, and hydrophobicity properties of diamond-like carbon films prepared by an anode layer source. *Mater. Res. Express.* **2019**, *6*, 055601. [CrossRef]
24. Meškinis, Š.; Vasiliauskas, A.; Andrulevičius, M.; Peckus, D.; Tamulevičius, S.; Viskontas, K. Diamond Like Carbon Films Containing Si: Structure and Nonlinear Optical Properties. *Materials* **2020**, *13*, 1003. [CrossRef] [PubMed]
25. Qi, M.; Xiao, J.; Cheng, Y.; Wang, Z.; Jiang, A.; Guo, Y.; Tao, Z. Effect of various nitrogen flow ratios on the optical properties of (Hf:N)-DLC films prepared by reactive magnetron sputtering. *AIP Adv.* **2017**, *7*, 085012. [CrossRef]
26. Kijaszek, W.; Wiatrowski, A.; Mazur, M.; Wojcieszak, D.; Paszkiewicz, R.; Kovac, J., Jr. Study on properties of diamond-like carbon films deposited by RF ICP PECVD method for micro- and optoelectronic applications. *Mater. Sci. Eng. B* **2023**, *296*, 116691. [CrossRef]
27. Boubiche, N.; El Hamouchi, J.; Hulik, J.; Abdesslam, M.; Speisser, C.; Djeffal, F.; Le Normand, F. Kinetics of graphitization of thin diamond-like carbon (DLC) films catalyzed by transition metal. *Diam. Relat. Mater.* **2019**, *91*, 190–198. [CrossRef]
28. Dovydaitis, V.; Marcinauskas, L.; Ayala, P.; Gnecco, E.; Chimborazo, J.; Zhairabany, H.; Zabels, R. The Influence of Cr and Ni Doping on the Microstructure of Oxygen Containing Diamond-like Carbon Films. *Vacuum* **2021**, *191*, 110351. [CrossRef]
29. Zhairabany, H.; Khaksar, H.; Vanags, E.; Marcinauskas, L. Effect of Molybdenum Concentration and Deposition Temperature on the Structure and Tribological Properties of the Diamond-like Carbon Films. *Crystals* **2024**, *14*, 962. [CrossRef]
30. Park, Y.S.; Jung, T.H.; Lim, D.G.; Park, Y.; Kim, H.; Choi, W.S. Tribological properties of metal doped a-C film by RF magnetron sputtering method. *Mater. Res. Bull.* **2012**, *47*, 2784–2787. [CrossRef]
31. Wu, Z.; Tian, X.; Gui, G.; Gong, C.; Yang, S.; Chu, P.K. Microstructure and surface properties of chromium-doped diamond-like carbon thin films fabricated by high power pulsed magnetron sputtering. *Appl. Surf. Sci.* **2013**, *276*, 31–36. [CrossRef]
32. Jastrzębski, K.; Grabarczyk, J.; Niedzielski, P.; Jędrzejczak, A.; Sobczyk-Guzenda, A.; Szymański, W.; Kamińska, M.; Skibska, B. The Doping of a Carbon Coating with Phosphorus as a Potential Way of Improving the Biological Properties of Diamond-like Carbon. *Materials* **2024**, *17*, 5859. [CrossRef]
33. Dong, H.; He, S.; Wang, X.; Zhang, C.; Sun, D. Study on conductivity and corrosion resistance of N-doped and Cr/N co-doped DLC films on bipolar plates for PEMFC. *Diam. Relat. Mater.* **2020**, *110*, 108156. [CrossRef]

34. Li, Z.; Ma, G.; Zhang, Z.; Shi, J.; He, T.; Han, C.; Xing, Z.; Wang, H. Vacuum tribological properties in Cr-doped H-DLC self-lubricating radial spherical plain bearings. *Diam. Relat. Mater.* **2024**, *141*, 110694. [CrossRef]
35. Písařík, P.; Jelínek, M.; Kocourek, T.; Zezulová, M.; Remsa, J.; Jurek, K. Chromium-doped diamond-like carbon films deposited by dual-pulsed laser deposition. *Appl. Phys. A* **2014**, *117*, 83–88. [CrossRef]
36. Mi, B.; Wang, H.; Wang, Q.; Cai, J.; Qin, Z.; Chen, Z. Corrosion resistance and contact resistance properties of Cr-doped amorphous carbon films deposited under different carbon target current on the 316L stainless steel bipolar plate for PEMFC. *Vacuum* **2022**, *203*, 111263. [CrossRef]
37. Savchenko, D.; Vorlíček, V.; Prokhorov, A.; Kalabukhova, E.; Lančok, J.; Jelínek, M. Raman and EPR spectroscopic studies of chromium-doped diamond-like carbon films. *Diam. Relat. Mater.* **2018**, *83*, 30–37. [CrossRef]
38. Assembayeva, A.; Ryaguzov, A.; Nemkayeva, R.; Guseinov, N.; Myrzabekova, M. Research of the structure of a-C films by the Raman spectroscopy method. *Mater. Today Proc.* **2019**, *25*, 58–63. [CrossRef]
39. Evaristo, M.; Azevedo, R.; Palacio, C.; Cavaleiro, A. Influence of the silicon and oxygen content on the properties of non-hydrogenated amorphous carbon coatings. *Diam. Relat. Mater.* **2016**, *70*, 201–210. [CrossRef]
40. Mi, B.; Wang, Q.; Xu, Y.; Qin, Z.; Chen, Z.; Wang, H. Improvement in Corrosion Resistance and Interfacial Contact Resistance Properties of 316L Stainless Steel by Coating with Cr, Ti Co-Doped Amorphous Carbon Films in the Environment of the PEMFCs. *Molecules* **2023**, *28*, 2821. [CrossRef]
41. Braca, E.; Saraceni, G.; Kenny, J.M.; Lozzi, L.; Santucci, S. Structural and optical properties of nitrogen and oxygen doped a-C:H coatings. *Thin Solid Films* **2002**, *415*, 195–200. [CrossRef]
42. Mikhchin, A.; Hosseini, S.I.; Abadi, S.K.N.; Mohammadhosseini, B.; Mehrabian, S. Tuning the optical, electrical, and structural properties of Cu-DLC thin films via simultaneous DC-RF unbalanced magnetron sputtering. *Heliyon* **2024**, *10*, e40171. [CrossRef] [PubMed]
43. Kundoo, S.; Kar, S. Nitrogen and Boron Doped Diamond Like Carbon Thin Films Synthesis by Electrodeposition from Organic Liquids and Their Characterization. *Adv. Mater. Phys. Chem.* **2013**, *3*, 25–32. [CrossRef]